



**University of
Zurich**^{UZH}

**Zurich Open Repository and
Archive**

University of Zurich
University Library
Strickhofstrasse 39
CH-8057 Zurich
www.zora.uzh.ch

Year: 2016

**Regulated protein depletion by the auxin-inducible degradation system in
*Drosophila melanogaster***

Trost, Martina ; Blattner, Ariane C ; Lehner, Christian F

DOI: <https://doi.org/10.1080/19336934.2016.1168552>

Posted at the Zurich Open Repository and Archive, University of Zurich

ZORA URL: <https://doi.org/10.5167/uzh-123934>

Journal Article

Accepted Version

Originally published at:

Trost, Martina; Blattner, Ariane C; Lehner, Christian F (2016). Regulated protein depletion by the auxin-inducible degradation system in *Drosophila melanogaster*. *Fly*, 10(1):35-46.

DOI: <https://doi.org/10.1080/19336934.2016.1168552>

1 **Regulated protein depletion by the auxin-inducible degradation system in**

2 *Drosophila melanogaster*

3

4 Martina Trost¹⁾, Ariane C. Blattner¹⁾, Christian F. Lehner^{1,2)}

5

6

7

8 1) Institute of Molecular Life Sciences (IMLS), University of Zurich, 8057 Zurich,

9 Switzerland

10 2) Author for correspondence (christian.lehner@imls.uzh.ch)

11

12 Keywords: protein degradation, protein depletion, auxin, inducible degradation, TIR1,

13 IAA17, auxin-dependent degron, auxin-inducible degradation, roughex

14

15 **Abstract**

16 The analysis of consequences resulting after experimental elimination of gene function has
17 been and will continue to be an extremely successful strategy in biological research.
18 Mutational elimination of gene function has been widely used in the fly *Drosophila*
19 *melanogaster*. RNA interference is used extensively as well. In the fly, exceptionally precise
20 temporal and spatial control over elimination of gene function can be achieved in
21 combination with sophisticated transgenic approaches and clonal analyses. However, the
22 methods that act at the gene and transcript level cannot eliminate protein products which are
23 already present at the time when mutant cells are generated or RNA interference is started.
24 Targeted inducible protein degradation is therefore of considerable interest for controlled
25 rapid elimination of gene function. To this end, a degradation system was developed in yeast
26 exploiting TIR1, a plant F box protein, which can recruit proteins with an auxin-inducible
27 degron to an E3 ubiquitin ligase complex, but only in the presence of the phytohormone
28 auxin. Here we demonstrate that the auxin-inducible degradation system functions efficiently
29 also in *Drosophila melanogaster*. Neither auxin nor TIR1 expression have obvious toxic
30 effects in this organism, and in combination they result in rapid degradation of a target
31 protein fused to the auxin-inducible degron.

32

33

34 **Introduction**

35 The stability of gene products often limits the speed of their experimental depletion.
36 Maternally contributed mRNA and protein can delay and blur the development of abnormal
37 phenotypes in progeny lacking zygotic function of a particular gene. Persistence of mRNA
38 and protein can also result in gradually changing phenotypes that sometimes impede accurate
39 interpretations after generation of mutant cells by mitotic recombination or comparable
40 approaches in clonal analyses. In case of RNA interference approaches, persistence of the
41 protein product can mask or delay manifestation of consequences. To circumvent such
42 problems, methods allowing regulated efficient degradation of specific target proteins have
43 been developed ¹.

44 In *Drosophila*, for example, expression of tobacco etch virus protease (TEV) for
45 degradation of a TEV-cleavable Rad21/Vtd variant, a functional cohesin complex subunit,
46 has been shown to result in an apparent null phenotype within the first cell cycle after the
47 onset of TEV expression when expressed instead of endogenous Rad21/Vtd ². TEV is also
48 exploited in a more versatile strategy involving the N-terminal TIPI tag ³ that exposes a
49 destabilizing N-terminus after TEV cleavage followed by degradation via the N-end rule
50 pathway ⁴. The N end rule pathway recognizes destabilizing N-terminal amino acids by a
51 dedicated ubiquitin ligase, resulting in polyubiquitylation and proteasomal degradation.
52 Interestingly, an N-end rule degron with temperature-sensitive activity has also been
53 developed ⁵ which has been applied in *Drosophila* to some limited extent ^{6,7}.

54 An elegant method (deGradFP) for targeted degradation of GFP fusion proteins involves
55 expression of a recombinant protein (NS1mb-vhh-GFP4) with an F-box fused to a camelid
56 single chain antibody against GFP ⁸. F-boxes mediate binding to Skp1, a component of E3
57 ubiquitin ligase complexes of the Skp1-Cullin-F-box (SCF) type. F-box proteins function as
58 substrate adaptors in these E3 complexes with the help of a second domain allowing specific

59 binding of target proteins. Thereby target proteins are recruited and polyubiquitylated,
60 followed by proteasomal degradation. Expression of NSlmb-vhh-GFP4 generates an SCF
61 ubiquitin ligase complex specific for GFP fusion proteins. This method for specific depletion
62 of GFP fusion proteins has been successfully applied in *Drosophila*⁸⁻¹¹.

63 While deGradFP acts at the protein level, it is neither particularly fast nor readily
64 reversible. NSlmb-vhh-GFP4 expressed from transgenes needs to accumulate to effective
65 intracellular concentrations that cannot be lowered again rapidly. For the induction of rapid
66 and reversible degradation, activity regulation of degrons by small chemicals is of great
67 interest. A few such controllable degrons have been developed¹. A most successful version¹²
68 is based on the molecular signaling mechanisms of the plant hormone auxin (indole-3-acetic
69 acid, IAA). In plants, auxin acts as molecular glue that mediates specific binding of
70 transcriptional repressors of the AUX/IAA family to the plant-specific F-box protein TIR1.
71 Auxin therefore results in polyubiquitylation and proteasomal degradation of these
72 transcriptional regulators¹³⁻¹⁵. The transcriptional repressors, including IAA17, contain an
73 auxin-inducible degron domain (AID) that is required and sufficient for binding to TIR1.
74 Heterologous TIR1 expression in yeast was demonstrated to result in association with
75 endogenous Skp1 and formation of a functional, auxin-dependent SCF ubiquitin ligase^{12, 16}.
76 Fusion proteins containing an AID are rapidly degraded in an auxin-dependent manner.
77 Beyond yeast, the auxin-inducible degradation system has been shown to function in
78 mammalian cells¹⁷, *Plasmodium*^{18, 19} and most recently even in the complex metazoan
79 model organism *Caenorhabditis elegans*²⁰. Here, we report that this system also functions
80 well in *Drosophila melanogaster* and describe transgenic strains for its application.

81

82

83 **Results and Discussion**

84 As a first step in our evaluation of the functionality of the auxin-dependent degradation
85 system in *Drosophila*, we addressed whether auxin might have adverse effects on cultured
86 cells. A suspension of S2R+ cells was distributed into multiwell plates and 24 hours later
87 auxin in increasing concentrations was added to the culture medium (final concentration 0,
88 0.3, 0.6, and 1 mM). Time lapse imaging was used to monitor cells over the next three days.
89 Even at the highest concentration we did not observe obvious effects on cell morphology and
90 cell numbers (Fig 1A, data not shown). In a second experiment, cells were harvested from
91 replicate cultures each day after auxin addition and used for determination of cell numbers
92 and viability (Fig. 1B). While 0.3 mM auxin did not have a significant effect, 1 mM reduced
93 cell doubling time slightly by about 10% compared to control cells growing in the absence of
94 auxin. Adverse effects on cell viability were not observed even at the highest concentration (1
95 mM). To evaluate whether auxin might affect *Drosophila* development, we collected eggs
96 from a *w¹* strain into vials with food containing auxin at different concentrations (0, 0.3, 0.6,
97 and 1 mM). From all the vials, adult flies were observed to eclose in comparable numbers
98 over a comparable time span. Because of our interest in future applications of the auxin-
99 inducible degradation system during male meiosis, we specifically tested the fertility of males
100 that had developed in the presence of increasing concentrations of auxin. We did not observe
101 any adverse effects of auxin onto male fertility. We conclude that auxin is not acutely toxic
102 for *Drosophila melanogaster* at the concentrations analyzed. Consistent with our
103 observations, previous analyses have failed to detect mutagenic effects of auxin after feeding
104 *Drosophila* larvae with concentrations up to 20 mM²¹.

105 To confirm that auxin actually penetrates into cultured S2R+ cells, we generated a test
106 construct for transient transfection experiments (Fig. 2A). This construct (pMT-OsTIR1-
107 P2A-H2B-aid-eyfp) allowed expression of rice TIR1 (OsTIR1) coupled via a "self-cleaving"

108 2A peptide²² to human histone H2B fused to the auxin-inducible degradation domain (aid)
109 and yellow fluorescent protein (eyfp). After transfection and induction of expression from the
110 construct, strong nuclear YFP signals were observed in transfected cells (Fig. 2B).
111 Reassuringly, these signals were no longer observed when cells were fixed 3 hours after
112 addition of auxin (1 mM) (Fig. 2B). Moreover, time lapse imaging confirmed that the strong
113 nuclear YFP signals vanished within 1 hour after auxin addition (Fig. 2C). We conclude that
114 auxin penetrates readily into Drosophila cells to reach concentrations capable of inducing
115 degradation of proteins with an auxin-inducible degradation domain.

116 To demonstrate the functionality of the auxin-inducible degradation system in the
117 organism, we generated transgenic Drosophila strains. A first construct was used for
118 generation of *UAS-OsTIR1* transgenic strains allowing GAL4-dependent expression of
119 OsTIR1. In addition, we generated *Ubi-OsTIR1* strains expressing OsTIR1 ubiquitously
120 under control of the *Ubi-p63E* promoter. Finally, we generated *UAS-aid-rux* strains allowing
121 GAL4-dependent expression of the auxin-inducible domain fused to Roughex. Drosophila
122 *roughex* (*rux*) codes for a Cdk inhibitor^{23, 24}. *rux* overexpression is known to interfere with
123 normal cell proliferation²³. We observed that the fusion protein Aid-Rux also caused severe
124 developmental abnormalities after expression of *UAS-aid-rux* with various tissue-specific
125 GAL4 drivers (*ey-GAL4*, *GMR-GAL4*, and *MS1096*) or lethality with more global drivers
126 (*Act5C-GAL4* and *en-GAL4*). To evaluate the auxin-dependent degradation system, we
127 crossed males with *UAS-aid-rux* and either *UAS-OsTIR1* or *Ubi-OsTIR1* with *en-GAL4*
128 virgin females. From these crosses, eggs were collected into vials with fly food that either did
129 or did not contain 1 mM auxin. After incubation of the vials at 25°C, we counted the number
130 of pupae and adult flies that developed. In the experiments with *Ubi-OsTIR1*, the number of
131 pupae was lower in the absence of auxin (287 without and 346 with auxin). Moreover, not a
132 single adult fly was observed to eclose in the absence of auxin, while in the presence of auxin

133 eight flies developed to the adult stage (Fig. 3A). However, all these adults displayed
134 morphological abnormalities most prominently in the wings. Often one of the two wings was
135 missing. The wings that were present had reduced posterior compartments (Fig. 3B). In
136 contrast, the wings of flies with only *en-GAL4* or only *UAS_t-aid-rux* and *Ubi-OsTIR1* were
137 entirely normal (data not shown).

138 In the experiments with *UAS-OsTIR1*, the protecting effect of auxin against *aid-rux*-
139 induced lethality was more prominent. In the presence of auxin, more pupae (294 without and
140 452 with auxin) and far more adult flies (0 without and 61 with auxin) were obtained
141 compared to absence of auxin (Fig. 3A). Those adult flies with *UAS_t-OsTIR1* that were
142 obtained in the presence of auxin were more normal than the few obtained with *Ubi-OsTIR1*.
143 But also in the *UAS_t-OsTIR1* case, adult wings were not entirely normal (Fig. 3C).
144 Abnormalities were more severe after development in lower concentrations of auxin (0.3 mM
145 compared to 1 mM) (Fig. 3C). Instead of the regular pattern of wing hairs, a multiple wing
146 hair phenotype was observed in the posterior compartment. During normal development,
147 each cell within the dorsal and ventral wing epithelium produces a single wing hair. We have
148 previously shown that Cdk1 inhibition specifically during the pupal stages disturbs the
149 formation of a single wing hair per cell²⁵. After Cdk1 inhibition during the pupal stages,
150 wing imaginal disc cells progress through endoreduplication cycles instead of going through
151 the two final mitotic cell cycles. The resulting oversized cells produce multiple instead of a
152 single wing hairs during terminal differentiation²⁵. The presence of a multiple wing hair
153 phenotype in the posterior compartment of *en-GAL4>UAS_t-aid-rux*, *UAS_t-OsTIR1* flies
154 indicates that the levels of auxin appear to drop to an ineffective concentration after
155 termination of auxin food uptake at the onset of larval wandering for preparation of
156 pupariation at the end of the third larval instar. In addition, the finding that adult flies were

157 only obtained in the presence of auxin strongly suggested that the auxin-inducible
158 degradation system is functional in *Drosophila*.

159 To study the effects of the auxin-induced degradation system more immediately at the
160 cellular level, we analyzed wing imaginal discs. After development of *en-GAL4* larvae with
161 *UAS-aid-rux* and either *UAS-OsTIR1* or *Ubi-OsTIR1* in the absence of auxin, the posterior
162 compartment was found to be strongly abnormal (Fig. 4A). DNA staining revealed the
163 presence of highly endoreduplicated cells within the posterior compartment. Moreover, the
164 overall shape of the disc was distorted to a variable extent. Development in the presence of
165 auxin prevented these abnormalities (Fig. 4A).

166 To analyze the dynamics of auxin-induced degradation in further detail, we generated
167 larvae carrying the transgenes *en-GAL4*, *UAS-OsTIR1* and *UAS-aid-rux*, as well as *tubP-*
168 *GAL80^{ts}* (Fig. 4B). Growing these larvae initially at 18°C prevented cells within the posterior
169 compartment from becoming highly abnormal in the absence of auxin. Expression of *UAS-*
170 *OsTIR1* and *UAS-aid-rux* was then induced eventually during 24 hours by shifting the larvae
171 to 29°C. Thereafter larvae were transferred to liquid food that either did or did not contain
172 auxin. Wing discs were dissected and fixed at different time points after transfer to liquid
173 food. As expected, immunolabeling with anti-Rux clearly revealed the presence of Aid-Rux
174 in the posterior compartment at the onset of feeding with liquid food (Fig. 4B). Moreover,
175 double labeling with anti-Cyclin A revealed that the accumulation of Aid-Rux was paralleled
176 by the disappearance of Cyclin A (Fig. 4B), as previously reported²³. Importantly, in the
177 presence of auxin, the intensity of the anti-Rux signals were observed to drop rapidly. Signals
178 were reduced to 22% (± 13 s.d., $n = 17$ wing discs) and 0.5% (± 0.7 s.d., $n = 20$) after two and
179 four hours in liquid auxin food, respectively. Presumably because Cyclin A re-accumulation
180 is a comparatively slow process, we did not observe a converse recovery of anti-Cyclin A
181 signal intensities. In addition, somewhat unexpectedly, anti-Rux signal intensities also went

182 down in the absence of auxin (Fig. 4B) to 41% (\pm 12 s.d., n = 20) and 15% (\pm 8 s.d., n = 20)
183 after two and four hours, respectively. However, the reduction in the absence of auxin was
184 significantly less extensive than that in the presence of auxin at both time points ($p < 0.0001$,
185 *t*-test). We conclude that Aid-Rux has a limited stability even in the absence of auxin-induced
186 degradation. Moreover, auxin-induced degradation makes it highly unstable.

187 In principle, the limited stability of Aid-Rux in the absence of auxin observed in our
188 experiments might reflect an auxin-independent activity of OsTIR1 in *Drosophila*. To address
189 whether OsTIR1 might have auxin-independent activity, we performed additional
190 experiments with *en-GAL4*, *tub-GAL80^{ts}*, *UAS-aid-rux* larvae that had either a *UAS-OsTIR1*
191 or a *UAS-lacZ* transgene. After initial development at 18°C, *UAS* transgene expression was
192 again induced (24 hours at 29°C) before transfer to auxin containing liquid food. Signal
193 intensities obtained with anti-Rux at the onset of feeding with liquid food were comparable in
194 the *UAS-OsTIR1* and *UAS-lacZ* wing discs (Fig. 5), indicating that OsTIR1 does not have
195 substantial auxin-independent activity. In addition, analysis of the anti-Rux signal intensities
196 after two and four hours in liquid food provided further confirmation that auxin induces
197 OsTIR1-mediated degradation. The drop in signal intensity was far more drastic in the discs
198 expressing *UAS-OsTIR1* compared to those expressing *UAS-lacZ* (Fig. 5). We conclude that
199 the auxin-dependent degradation system functions also in *Drosophila* as expected.

200 Our work indicates that the auxin-inducible degradation should be an attractive option for
201 spatially and temporally precise depletion of proteins of interest in *Drosophila melanogaster*.
202 Already the recent evaluation of this approach in *Caenorhabditis elegans*²⁰ has demonstrated
203 impressively that it functions not only in yeast and cultured cells but also in complex
204 metazoan organism. Moreover, the analyses in the nematode suggest interesting perspectives
205 for further improvements. Instead of the complete AID from IAA17 (229 amino acids) a
206 subregion of only 44 amino acids was shown to function as an efficient auxin-dependent

207 degran in the nematode. Moreover, it is readily conceivable that the TIR1 gene version from
208 *Arabidopsis thaliana* with two point mutations improving affinity and auxin sensitivity,
209 which has been used very successfully in the nematode, might perform better than rice TIR1
210 that was used in our experiments.

211

212 **Materials and Methods**

213 **Plasmids**

214 For the construction of pMT-OsTIR1-P2A-H2B-aid-eyfp we used a plasmid with an insert
215 coding for human histone H2B fused the auxin-inducible degradation domain (aid) and
216 enhanced yellow fluorescent protein (eyfp)¹⁷ as well as pNHK36 containing the OsTIR1
217 coding sequence¹² and pC5Kan-P2A (Addgene #5184)²². Primers AB108 (5'-TGCC
218 AGATCT ATGCCAGAGCCAGCGAAGTC-3') and AB109 (5'-CGGG ACGCGT
219 TCTAGATTACTTGTACAGCTCGTCCA-3') were used for enzymatic amplification of the
220 H2B-aid-eyfp fragment. After digestion with BglII and MluI the fragment was inserted into
221 the corresponding restriction sites of pC5-Kan-P2A. Into the Acc65I and SalI sites of the
222 resulting cloning intermediate, the OsTIR1 sequence was inserted after enzymatic
223 amplification with the primers AB110 (5'-ATCC GGTACC
224 ATGACGTACTTCCCGGAGGA-3') and AB111 (5'-ACCG GTCGAC
225 GCTAGGATTTTAACAAAATTTG-3') and digestion with the corresponding enzymes.
226 From this second cloning intermediate, the Os-TIR1-P2A-H2B-aid-eyfp fragment was
227 released with KpnI and XbaI, and inserted into pMT between the *MtnA* promoter²⁶ and the
228 SV40 terminator.

229 For the generation of pUAS_t-OsTIR1-K7, the OsTIR1 coding sequence was amplified with
230 the primers CL198 (5'-ACCGG GAATTC AAAATGACGTACTTCCCGGAGGAG-3') and
231 CL199 (5'-GGCC TCTAGA CTATAGGATTTTAACAAAATTTG-3'). After digestion with
232 EcoRI and XbaI, the fragment was inserted into a modified pUAS_t vector²⁷ in which a
233 shortened SV40 terminator (K7) was present instead of the original long SV40 terminator
234 region, which is known to trigger nonsense-mediated mRNA decay and hence reduced
235 expression²⁸

236 For the production of pWRpUbi-OsTIR1, the OsTIR1 coding region was amplified with
237 CL191 (5'-CGGA GGTACC AAAATGACGTACTTCCCGGAGGAG-3') and CL192 (5'-
238 GGCC GAATTC CTATAGGATTTTAACAAAATTTG-3'). After digestion with KpnI and
239 EcoRI, the fragment was inserted into the corresponding sites of pWRpUbiqPE. This places
240 the *OsTIR1* coding sequence downstream of the *Ubi-p63E* promoter and upstream of the
241 *rosy*⁺ terminator sequences. Moreover, the resulting construct contains the *w*^{+mC} marker gene,
242 as well as P element end sequences for *Drosophila* germline transformation.

243 For the production of UAS*t-aid-rux*, we amplified the *aid* coding region from pMT-
244 OsTIR1-P2A-H2B-*aid-eyfp* with the primers MT55 (5'-TGCC AGATCT
245 ATGGGCAGTGTCTGAGCT-3') (BglII) and MT56 (5'-ACGG ACGCGT
246 AGCTCTGCTCTTGCACCTTCTC-3'). After digestions with BglII and MluI, the PCR
247 fragment was cloned into the corresponding restriction sites of pC5Kan-P2A. Into the MluI
248 and NheI sites of the resulting cloning intermediate, a *rux* cDNA fragment containing the
249 complete coding sequence was inserted. This *rux* cDNA fragment was amplified first with
250 primers OL5 (5'-AGTAATTATTGAATACAAGAAGAG-3') and OL6 (5'-
251 GTCCAATTATGTACACCACAGAA-3') from genomic DNA isolated from the
252 *Drosophila UAS-rux* strain²³, followed by re-amplification with primers MT57 (5'-TGCC
253 ACGCGT ATGAGCGCTCCAGAAGAAC-3') and MT58 (5'-ACGG GCTAGC
254 GCGGCCGC CTAGAAACGCATCCGCC-3') and digestion with MluI and NheI. BglII and
255 NotI were used for the release of the *aid-rux* fragment from the second cloning intermediate.
256 The fragment was then inserted into the corresponding restriction sites of pUAS*t*.

257

258 ***Drosophila* strains and husbandry**

259 The following GAL4 driver transgenes were used: *P{en2.4-GAL4}e16E (en-GAL4)*²⁷,
260 *P{Act5C-GAL4}25FO1* (Y. Hiromi, unpublished), *P{GAL4-ey.H}*²⁹, *P{GAL4-*

261 *ninaE.GMR}12 (ey-GAL4)³⁰, P{GawB}Bx^{MS1096}³¹. For temperature dependent regulation of
262 *en-GAL4* driven expression with the help of *P{tubP-GAL80^{ts}}20 (tubP-GAL80^{ts})³²*, we used a
263 stock with a recombinant *en-GAL4, tubP-GAL80^{ts}* chromosome balanced over *CyO, P{Dfd-
264 GMR-nvYFP}³³*. Larvae lacking the balancer chromosome were selected using a
265 stereomicroscope equipped for fluorescence detection.*

266 Strains carrying the *UAS-OsTIRI* transgene on either chromosome II (II.1) or chromosome
267 III (III.1 and III.2) were generated with the construct described above. Insertion II.1 was used
268 for the experiments described here.

269 Strains carrying the *Ubi-OsTIRI* transgene on either chromosome II (II.1 and II.2) or III
270 (III.1) were generated with the construct described above. Insertion II.1 was used for the
271 experiments described here.

272 Strains carrying the *UAS-aid-rux* gene were generated with the construct described above.
273 Insertion III.1 was used in combination with *UAS-OsTIRI(II.1)*, as well as with *Ubi-
274 OsTIRI(II.1)*. Moreover, for control experiments, *UAS-aid-rux (III.1)* was combined with
275 *UAS-lacZ (II)³⁴*.

276 Flies were raised on standard food (100 g yeast, 75 g glucose, 55 g corn meal, 10 g wheat
277 flour, 8 g agar, 250 mg Nipagin, 1 L water). For addition of auxin, fly food was melted in a
278 microwave. After cooling to about 40°C, the required volume of auxin stock solution was
279 added followed by thorough mixing and solidification. The auxin stock solution was
280 generated by dissolving indole-3-acetic acid sodium salt (Sigma-Aldrich, I5148) at a
281 concentration of 1 M in water followed by sterile filtration. The stock solution was frozen in
282 aliquots at -20°C.

283 Liquid food for *Drosophila* larvae was prepared essentially as described³⁵. One liter of
284 liquid food contained 100 g of yeast extract, 100 glucose and 75 g sucrose dissolved in water.
285 The food was sterilized by filtration. Before transfer of larvae into liquid food, eggs were

286 collected from the appropriate crosses in fly bottles during 24 hours at 25°C. Parents were
287 discarded and bottles were incubated for seven days at 18°C. Subsequently, bottles were
288 transferred into a water bath within a 29°C incubator for an additional 24 hours. For the
289 isolation of larvae, 20% sucrose in water was added to the bottles containing fly food and
290 larvae. After gentle mixing, larvae floating on top were transferred into a basket with a nylon
291 mesh at the bottom. Excess sucrose solution was washed away with tap water. Baskets with
292 larvae were then transferred into petri dishes containing liquid food (0.95 mL) to which red
293 food color (0.04 mL) had been added just before, as well as auxin stock solution if required.
294 Final concentration of auxin was 1 mM if not specified otherwise. After larval feeding in
295 liquid food for the appropriate time period, the largest larvae with red guts were picked with
296 forceps, followed by dissection of wing imaginal discs in Schneider's tissue culture medium.
297

298 **Cell culture**

299 S2R+ cell culture, transfection and time lapse imaging were done essentially as previously
300 described³⁶. To assess auxin effects by time lapse imaging, 75,000 cells/well were plated in a
301 24 well plate. Auxin was added to the medium one day after plating. For each concentration
302 (0, 0.3, 0.6, and 1 mM), we started three replicate cultures. On the bottom of each well, one
303 position was marked. Phase contrast images were acquired next to the mark on consecutive
304 time points (t = 0, 5, 24, 48 and 72 hours) with a 20X/0.5 objective on a Zeiss Cell Observer
305 HS wide-field microscope. Replicate cultures displayed identical behavior as illustrated in
306 Fig. 1A. For the evaluation of auxin effects on cell numbers and viability, cells were plated
307 into 35 mm dishes. Auxin was again added to the medium one day after plating. Three
308 replicate cultures were started for each time point (0, 24, 48, and 72 hours after auxin
309 addition) and auxin concentration (0, 0.3, and 1 mM). Cells were harvested by trypsinization.
310 Trypan Blue was added and the numbers of live and dead cells were determined. For time

311 lapse imaging of H2B-aid-eyfp degradation, S2R+ cells were plated into 35 mm glass bottom
312 dishes and transfected with pMT-OsTIR1-P2A-H2B-aid-eyfp. 0.5 mM CuSO₄ was added 40
313 hours after transfection. Auxin (0.5 mM) was added 24 hours later. Culture replicates were
314 either fixed at different times after auxin addition or used for time lapse imaging. Images
315 were acquired using a 40x/1.30 oil immersion objective on a Zeiss Cell Observer HS wide-
316 field microscope.

317

318 **Immunofluorescence**

319 Wing imaginal discs were fixed in 4% formaldehyde for 20 minutes on a rotating wheel.
320 Subsequent staining was performed as described previously³⁷. For anti-Rux immunolabeling
321 we used a 1:1 mixture of hybridoma supernatants containing either mouse monoclonal
322 antibody H6 and H9, respectively,²³ that was further diluted 1:1.5. Rabbit antiserum against
323 *Drosophila* Cyclin A³⁸ was used at a dilution of 1:600. Rabbit anti-beta-Galactosidase (MP
324 Biomedicals, 0855976) was used at a dilution of 1:2000. For DNA labeling we used Hoechst
325 33258 at a final concentration of 1 µg/mL. Wing discs of larvae expressing either *UAS-lacZ*
326 or *UAS-OsTIR1* were pooled for fixation, staining and mounting. Image stacks with three
327 focal planes spaced by 500 nm were acquired with a 40x/1.30 oil immersion objective on a
328 Zeiss Cell Observer HS microscope. Anti-Rux signals were quantified after maximum
329 intensity projection using Image J. Regions of interest on both sides of the anterior-posterior
330 compartment boundary were selected before determination of average pixel intensity. Signals
331 in the anterior compartment were used for background correction. 17-20 wing discs for each
332 genotype and conditions were quantified in case of the experiments illustrated in Fig. 4B, and
333 three imaginal discs in case of Fig. 5.

334

335 **Acknowledgements**

336 We thank M. Kanemaki and E. Caussinus for material and advice, as well as L. Zipursky for
337 monoclonal antibodies against Rux, and S. Moser for technical support. This work was
338 supported by the Swiss National Science Foundation (grant 31003A_120276 to C.F.L.).
339

340 **References**

- 341 1. Kanemaki MT. Frontiers of protein expression control with conditional degrons.
342 Pflugers Arch 2013; 465:419-25.
- 343 2. Pauli A, Althoff F, Oliveira RA, Heidmann S, Schuldiner O, Lehner CF, Dickson BJ,
344 Nasmyth K. Cell-type-specific TEV protease cleavage reveals cohesin functions in
345 Drosophila neurons. Dev Cell 2008; 14:239-51.
- 346 3. Taxis C, Knop M. TIPI: TEV protease-mediated induction of protein instability.
347 Methods Mol Biol 2012; 832:611-26.
- 348 4. Varshavsky A. The N-end rule pathway and regulation by proteolysis. Protein science :
349 a publication of the Protein Society 2011; 20:1298-345.
- 350 5. Dohmen RJ, Wu P, Varshavsky A. Heat-inducible degron: a method for constructing
351 temperature-sensitive mutants. Science 1994; 263:1273-6.
- 352 6. Speese SD, Trotta N, Rodesch CK, Aravamudan B, Broadie K. The ubiquitin
353 proteasome system acutely regulates presynaptic protein turnover and synaptic efficacy.
354 Curr Biol 2003; 13:899-910.
- 355 7. Nicholson SC, Nicolay BN, Frolov MV, Moberg KH. Notch-dependent expression of
356 the archipelago ubiquitin ligase subunit in the Drosophila eye. Development 2011;
357 138:251-60.
- 358 8. Caussinus E, Kanca O, Affolter M. Fluorescent fusion protein knockout mediated by
359 anti-GFP nanobody. Nat Struct Mol Biol 2011; 19:117-21.
- 360 9. Raychaudhuri N, Dubruille R, Orsi GA, Bagheri HC, Loppin B, Lehner CF.
361 Transgenerational propagation and quantitative maintenance of paternal centromeres
362 depends on Cid/Cenp-A presence in Drosophila sperm. PLoS Biol 2013; 10:e1001434.

- 363 10. Urban E, Nagarkar-Jaiswal S, Lehner CF, Heidmann SK. The cohesin subunit Rad21 is
364 required for synaptonemal complex maintenance, but not sister chromatid cohesion,
365 during *Drosophila* female meiosis. *PLoS Genet* 2014; 10:e1004540.
- 366 11. Bätz T, Förster D, Luschnig S. The transmembrane protein Macroglobulin
367 complement-related is essential for septate junction formation and epithelial barrier
368 function in *Drosophila*. *Development* 2014; 141:899-908.
- 369 12. Nishimura K, Fukagawa T, Takisawa H, Kakimoto T, Kanemaki M. An auxin-based
370 degron system for the rapid depletion of proteins in nonplant cells. *Nat Methods* 2009;
371 6:917-22.
- 372 13. Dharmasiri N, Dharmasiri S, Estelle M. The F-box protein TIR1 is an auxin receptor.
373 *Nature* 2005; 435:441-5.
- 374 14. Kepinski S, Leyser O. The *Arabidopsis* F-box protein TIR1 is an auxin receptor. *Nature*
375 2005; 435:446-51.
- 376 15. Tan X, Calderon-Villalobos LI, Sharon M, Zheng C, Robinson CV, Estelle M, Zheng
377 N. Mechanism of auxin perception by the TIR1 ubiquitin ligase. *Nature* 2007; 446:640-
378 5.
- 379 16. Kanke M, Nishimura K, Kanemaki M, Kakimoto T, Takahashi TS, Nakagawa T,
380 Masukata H. Auxin-inducible protein depletion system in fission yeast. *BMC Cell Biol*
381 2011; 12:8.
- 382 17. Holland AJ, Fachinetti D, Han JS, Cleveland DW. Inducible, reversible system for the
383 rapid and complete degradation of proteins in mammalian cells. *Proc Natl Acad Sci U S S*
384 *A* 2012; 109:E3350-7.
- 385 18. Kreidenweiss A, Hopkins AV, Mordmuller B. 2A and the auxin-based degron system
386 facilitate control of protein levels in *Plasmodium falciparum*. *PLoS One* 2013;
387 8:e78661.

- 388 19. Philip N, Waters AP. Conditional Degradation of Plasmodium Calcineurin Reveals
389 Functions in Parasite Colonization of both Host and Vector. *Cell Host Microbe* 2015;
390 18:122-31.
- 391 20. Zhang L, Ward JD, Cheng Z, Dernburg AF. The auxin-inducible degradation (AID)
392 system enables versatile conditional protein depletion in *C. elegans*. *Development*
393 2015; 142:4374-84.
- 394 21. Karadeniz A, Kaya B, Savas B, Topcuoglu SF. Effects of two plant growth regulators,
395 indole-3-acetic acid and beta-naphthoxyacetic acid, on genotoxicity in *Drosophila*
396 SMART assay and on proliferation and viability of HEK293 cells from the perspective
397 of carcinogenesis. *Toxicol Industr Health* 2011; 27:840-8.
- 398 22. Daniels RW, Rossano AJ, Macleod GT, Ganetzky B. Expression of multiple transgenes
399 from a single construct using viral 2A peptides in *Drosophila*. *PLoS One* 2014;
400 9:e100637.
- 401 23. Thomas BJ, Zavitz KH, Dong XZ, Lane ME, Weigmann K, Finley RL, Brent R, Lehner
402 CF, Zipursky SL. roughex down-regulates G2 cyclins in G1. *Genes Dev* 1997;
403 11:1289-98.
- 404 24. Foley E, O'Farrell PH, Sprenger F. Rux is a cyclin-dependent kinase inhibitor (CKI)
405 specific for mitotic cyclin-Cdk complexes. *Curr Biol* 1999; 9:1392-402.
- 406 25. Weigmann K, Cohen SM, Lehner CF. Cell cycle progression, growth and patterning in
407 imaginal discs despite inhibition of cell division after inactivation of *Drosophila* Cdc2
408 kinase. *Development* 1997; 124:3555-63.
- 409 26. Bunch TA, Grinblat Y, Goldstein LS. Characterization and use of the *Drosophila*
410 metallothionein promoter in cultured *Drosophila melanogaster* cells. *Nucleic Acids Res*
411 1988; 16:1043-61.

- 412 27. Brand AH, Perrimon N. Targeted gene expression as a means of altering cell fates and
413 generating dominant phenotypes. *Development* 1993; 118:401-15.
- 414 28. Metzstein MM, Krasnow MA. Functions of the nonsense-mediated mRNA decay
415 pathway in *Drosophila* development. *PLoS Genet* 2006; 2:e180.
- 416 29. Hazelett DJ, Bourouis M, Walldorf U, Treisman JE. decapentaplegic and wingless are
417 regulated by eyes absent and eyegone and interact to direct the pattern of retinal
418 differentiation in the eye disc. *Development* 1998; 125:3741-51.
- 419 30. Freeman M. Reiterative use of the EGF receptor triggers differentiation of all cell types
420 in the *Drosophila* eye. *Cell* 1996; 87:651-60.
- 421 31. Capdevila J, Guerrero I. Targeted expression of the signaling molecule decapentaplegic
422 induces pattern duplications and growth alterations in *Drosophila* wings. *EMBO J*
423 1994; 13:4459-68.
- 424 32. McGuire SE, Le PT, Osborn AJ, Matsumoto K, Davis RL. Spatiotemporal rescue of
425 memory dysfunction in *Drosophila*. *Science* 2003; 302:1765-8.
- 426 33. Le T, Liang Z, Patel H, Yu MH, Sivasubramaniam G, Slovitt M, Tanentzapf G,
427 Mohanty N, Paul SM, Wu VM, et al. A new family of *Drosophila* balancer
428 chromosomes with a w- dfd-GMR yellow fluorescent protein marker. *Genetics* 2006;
429 174:2255-7.
- 430 34. Fischer JA, Giniger E, Maniatis T, Ptashne M. GAL4 activates transcription in
431 *Drosophila*. *Nature* 1988; 332:853-6.
- 432 35. Gasque G, Conway S, Huang J, Rao Y, Vosshall LB. Small molecule drug screening in
433 *Drosophila* identifies the 5HT2A receptor as a feeding modulation target. *Scientific*
434 *reports* 2013; 3:srep02120.
- 435 36. Lidsky PV, Sprenger F, Lehner CF. Distinct modes of centromere protein dynamics
436 during cell cycle progression in *Drosophila* S2R+ cells. *J Cell Sci* 2013; 126:4782-93.

- 437 37. Handke B, Szabad J, Lidsky PV, Hafen E, Lehner CF. Towards long term cultivation of
438 *Drosophila* wing imaginal discs in vitro. PLoS One 2014; 9:e107333.
- 439 38. Sprenger F, Yakubovich N, O'Farrell PH. S phase function of *Drosophila* cyclin A and
440 its downregulation in G1 phase. Curr Biol 1997; 7:488-99.
- 441

442 **Figure legends**

443 **Figure 1.** Auxin effects on *Drosophila* S2R+ cells. To evaluate potential toxicity of auxin,
444 S2R+ cells were cultured in the presence of auxin at the indicated concentrations (mM). **(A)**
445 No obvious effects of auxin on cell morphology were observed by imaging defined regions
446 repeatedly at the indicated time points (hours) after auxin addition. Scale bar = 100 μ m. **(B)**
447 Cell counting revealed a slight inhibitory effect of 1 mM auxin on cell proliferation, while 0.3
448 mM did not appear to have a significant effect. Average cell numbers (+/- s.d., n = 3) at the
449 indicate time points (hours) after addition of auxin (0, 0.3 and 1 mM) are shown.

450

451 **Figure 2.** Auxin induced degradation in *Drosophila* S2R+ cells. **(A)** Scheme illustrating the
452 characteristic features of the pMT-OsTIR1-P2A-H2B-aid-eyfp construct and of the auxin-
453 inducible degradation system. The *MtnA* promoter (pMT) controls expression of an mRNA
454 that includes the sequence of a "self-cleaving" 2A peptide (P2A). Therefore, the mRNA
455 generates two distinct proteins. The first is the protein TIR1 from rice (OsTIR1) which
456 includes an F box (F) that allows integration into an SCF ubiquitin ligase complex together
457 with the endogenous *Drosophila* proteins Skp1, Cul1, Rbx1 and an E2 protein. The second
458 protein is a histone H2B fusion protein with a C terminal extension that consists of the auxin-
459 inducible degron (aid) followed by EYFP (eyfp). In the presence of auxin, aid-containing
460 proteins are recruited to OsTIR1, resulting in their polyubiquitinylation and proteasomal
461 degradation.

462 **(B)** The construct illustrated in panel A was transfected into S2R+ cells. Construct expression
463 was either induced (+ CuSO₄) or not induced (- CuSO₄) before fixation and imaging. The
464 strong nuclear YFP signals, which were observed in transfected and induced cells before
465 addition of auxin (t = 0), were no longer present when cells were fixed 3 hours after addition
466 of auxin (t = 3). Scale bar = 20 μ m. **(C)** By time lapse imaging the nuclear YFP signals were

467 confirmed to disappear from transfected and induced S2R+ cells within less than an hour
468 after addition of auxin. The upper images (t = 0) were acquired immediately before and the
469 lower images (t = 1) one hour after auxin addition.

470

471 **Figure 3.** Auxin and OsTIR1 expression suppress Aid-Rux induced lethality during
472 Drosophila development. (A) Schematic illustration of the experimental strategy used for the
473 evaluation of the auxin-inducible degradation system during Drosophila development. Eggs
474 with the indicated genotypes were collected on fly food with or without auxin. While
475 complete developmental lethality was observed in the absence of auxin, the indicated number
476 of adult flies eclosed in the presence of auxin. (B) The posterior wing compartments of *en-*
477 *GAL4>UASaid-rux, Ubi-OsTIR1* flies after development in the presence of auxin were
478 observed to be severely reduced. (C) The posterior wing compartments of *en-GAL4>UAS-*
479 *aid-rux, UAS-OsTIR1* flies after development in the presence of auxin were observed to be
480 abnormal as well. Abnormalities were more severe after development in the presence of 0.3
481 mM compared to 1 mM auxin. While the size of the posterior compartment was usually close
482 to normal, it displayed a multiple wing hair phenotype, as clearly apparent in the high
483 magnification view on the right. Scale bar = 0.4 mm.

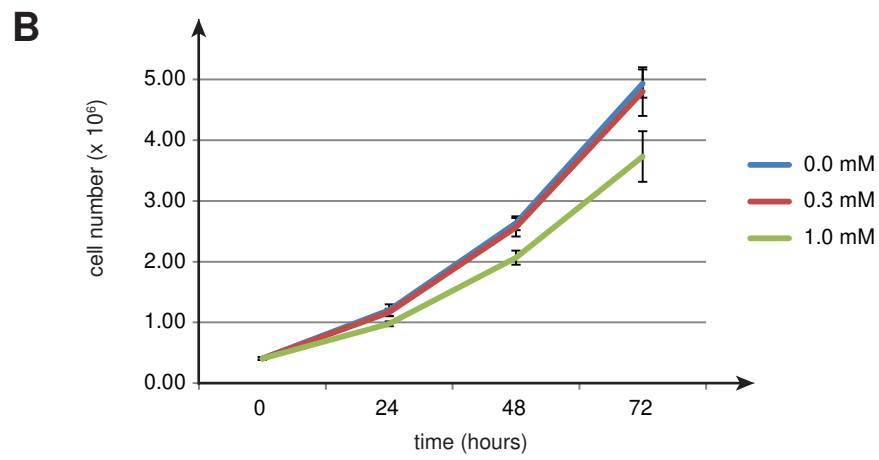
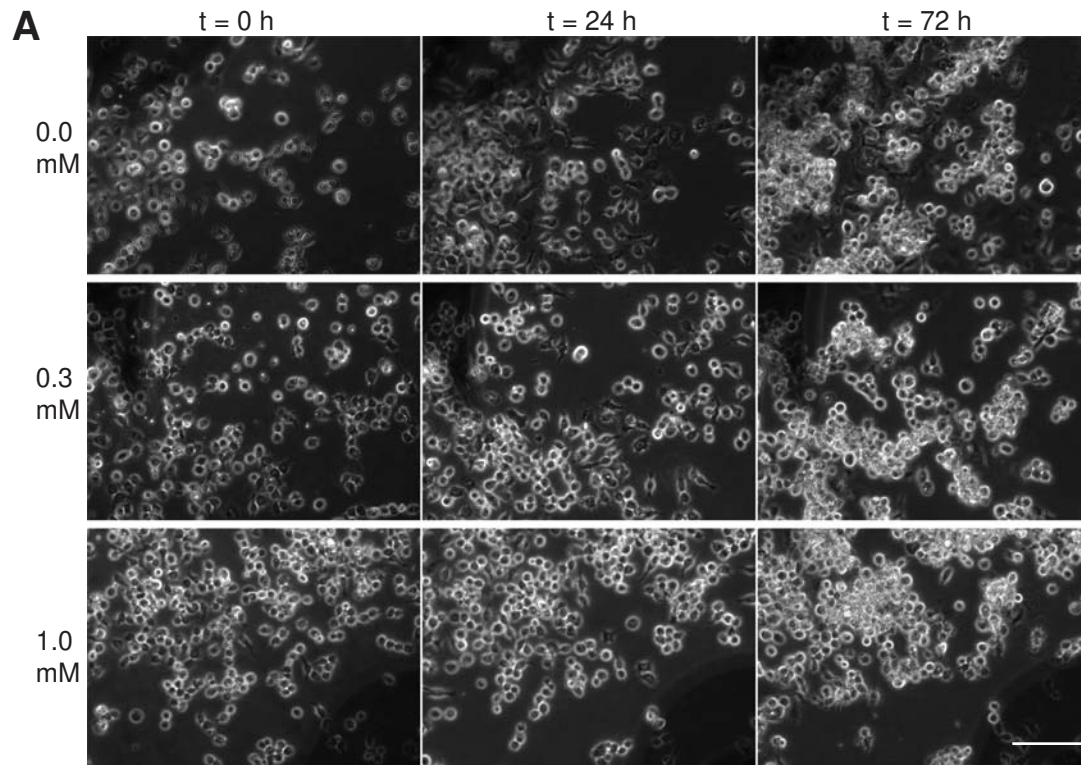
484

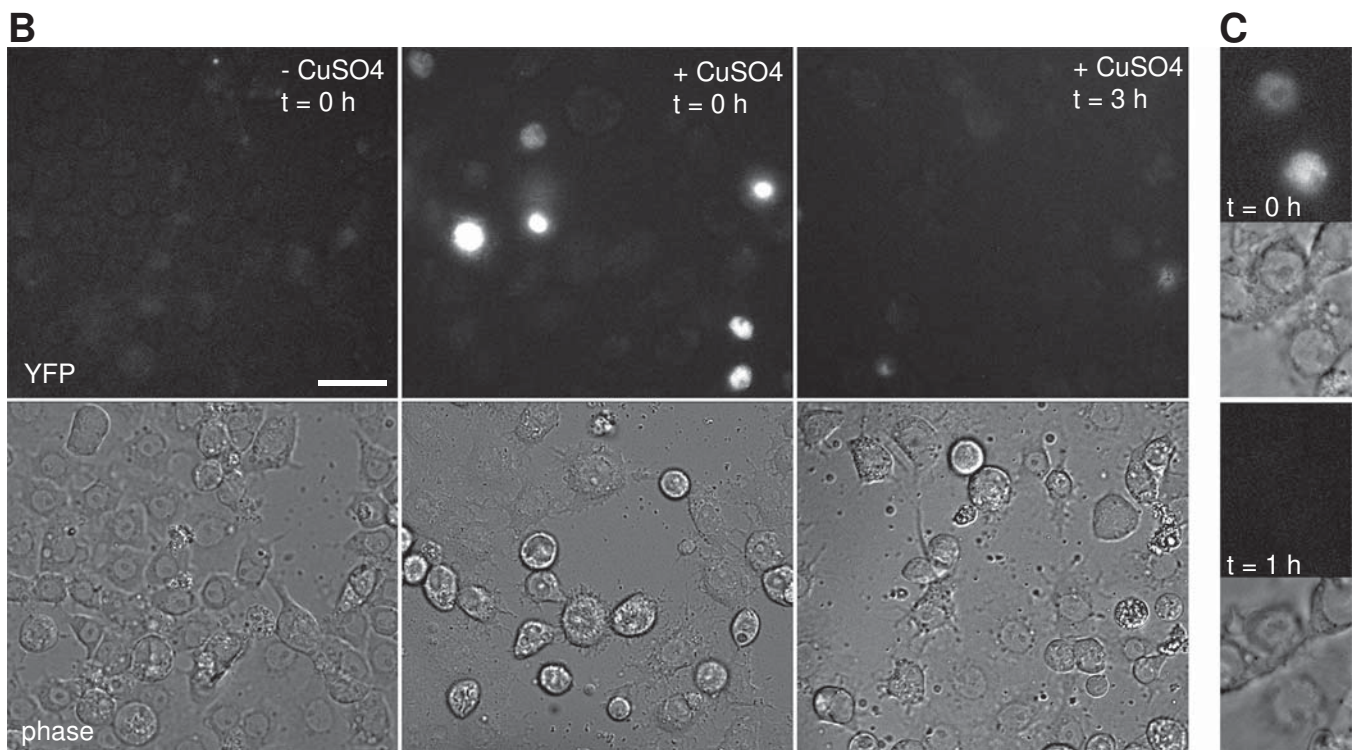
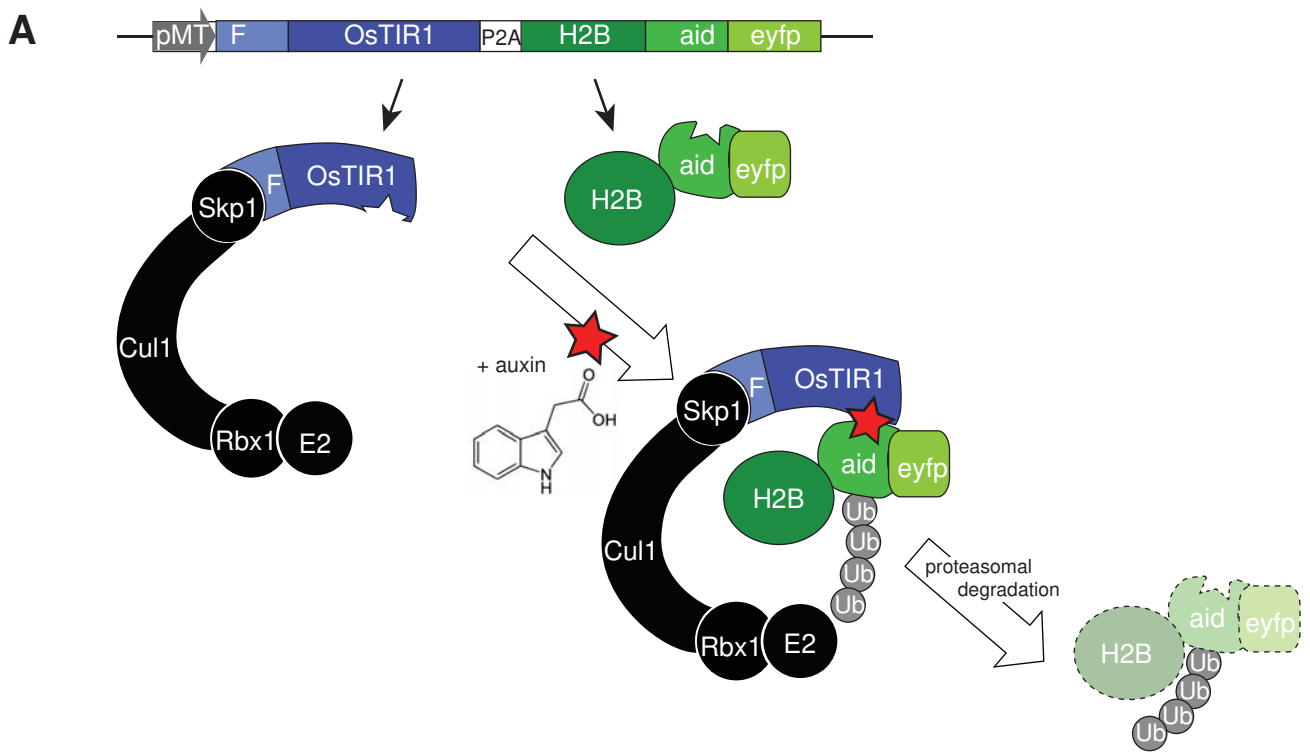
485 **Figure 4.** Aid-Rux depletion by auxin and OsTIR1 expression suppresses endoreduplication
486 in wing discs. (A) Wing imaginal discs from third instar wandering stage larvae with *en-*
487 *GAL4>UASaid-rux* and either *UAS-OsTIR1* or *Ubi-OsTIR1*, as indicated, were fixed after
488 development in the absence (-) or presence (+) of auxin. DNA staining revealed
489 endoreduplicated nuclei at lower density in the posterior wing disc compartment of larvae
490 grown in the absence of auxin. Boxed regions are shown at higher magnification in the
491 bottom panels. The effects of *aid-rux* expression in the posterior compartment resulted in

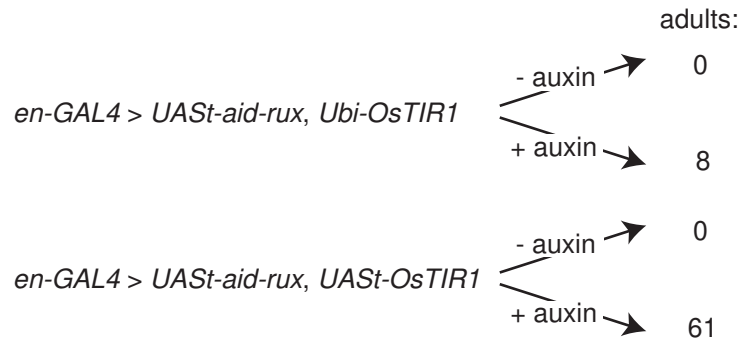
492 variable distortions of the wing imaginal discs, as evident in the example shown in the
493 leftmost panel where the posterior compartment runs oblique across the disc. Scale bar = 50
494 μm . **(B)** Larvae with *en-GAL4, tubP-GAL80^{ts}>UAS^t-aid-rux, UAS^t-OsTIR1* were grown
495 initially at 18°C. GAL4-mediated expression of the *UAS^t* transgenes was induced for 24
496 hours at 29°C. Larvae were then transferred into liquid food without (- auxin) or with (+
497 auxin) auxin for the indicated time (hours). Wing imaginal discs were dissected and stained
498 with anti-Rux, anti-Cyclin A and a DNA stain. Wing pouch regions with anterior and
499 posterior compartment on the left and right side, respectively, are shown. Aid-Rux is
500 degraded more rapidly in the presence of auxin. Scale bar = 10 μm .

501

502 **Figure 5.** OsTIR1 does not cause auxin-independent Aid-Rux degradation. **(A)** *en-GAL4,*
503 *tubP-GAL80^{ts}>UAS^t-aid-rux* larvae with either *UAS^t-lacZ* or *UAS^t-OsTIR1*, as indicated,
504 were grown initially at 18°C. GAL4-mediated expression of the *UAS^t* transgenes was induced
505 for 24 hours at 29°C. Larvae were then transferred for the indicated time (hours) into auxin
506 containing liquid food. Wing imaginal discs were dissected and stained with anti-Rux and a
507 DNA stain. OsTIR1 does not lower Aid-Rux levels before addition of auxin but results in
508 rapid degradation after addition of auxin. Scale bar = 20 μm . **(B)** Anti-Rux signals in the
509 posterior compartment of wing discs obtained in the experiment illustrated in (A) were
510 quantified. Average signals were normalized with those observed in *en-GAL4, tubP-*
511 *GAL80^{ts}>UAS^t-aid-rux, UAS^t-lacZ* which were set to 100%; whiskers indicate s.d. (n = 3),
512 *** p = 0.00013 (*t*-test).





A**B** *Ubi-OsTIR1*, + auxin**C** *UAS_{OsTIR1}*, + auxin